

# On the covariance of scan-matching techniques for localization

Silvère Bonnabel, Martin Barczyk and François Goulette

**Abstract**—This paper considers the problem of estimating the covariance of the relative displacement measurement output by the Iterative Closest Point (ICP) algorithm. The problem is relevant for localization of mobile robots (using a sensor of the Kinect type) or for autonomous vehicles (using a sensor of the Velodyne type) where the relative displacement measurement must be fused with other sensors’ measurements, such as wheel encoders or inertial sensors, in a Kalman or a particle filter. The closed-form formulas proposed in previous literature generally build upon the fact that the solution to ICP is obtained by minimizing a function of the data. In this paper, we prove this approach is on shaky ground because the rematching step of the ICP is not explicitly accounted for, and a blind application to point-to-point ICP leads to completely erroneous covariances. Yet we justify that the method is applicable to point-to-plane ICP as already known to practitioners, by proposing a geometric mathematical proof bounding the errors made.

## I. INTRODUCTION

This paper considers the covariance of estimates obtained by applying the Iterative Closest-Point (ICP) algorithm [1], [2] to pairs of successive point clouds captured by a scanning sensor moving through a structured environment. This so-called scan matching [3] allows to estimate the relative change in pose of a robot carrying the scanner in either 2D (heading  $R \in SO(2)$  and in-plane position  $p \in \mathbb{R}^2$ ) or 3D (attitude  $R \in SO(3)$  and position  $p \in \mathbb{R}^3$ ).

### A. Motivations

In mobile robotics, and more generally for autonomous navigation, one seeks to estimate the vehicle’s pose (localization), or pose and surrounding landmarks (simultaneous localization and mapping or SLAM). For either of these cases, it may prove useful to fuse these estimates with other sensors’ readings, such as odometry, visual landmark detection, and/or GPS. We think in particular here to the realm of so-called Pose SLAM, or more generally Graph-based SLAM (see e.g. [4]) where relative displacements between two (possibly remote) poses of the robot allow to add edges in the graph and eventually refine the localization. In any case, to apply probabilistic filtering and sensor fusion techniques such as the extended Kalman filter (EKF) e.g. [5], [6], EKF variants, particle filtering methods, or optimization-based smoothing techniques to find a maximum likelihood estimate as in Graph SLAM, the probability distribution of the sensor’s error is required. Since in practice the noise

is typically assumed to be centered and Gaussian, only a covariance matrix is needed.

Contrarily to conventional localization sensors, the covariance of relative displacement estimates will not only depend on the sensor’s own noise but also on the geometry of the environment. Indeed, when it comes to scan matching with ICP several sources of errors come into play.

- 1) the presence of geometry in one scan not observed in the subsequent one(s), that is, lack of overlapping
- 2) mismatching of points, that is, both scans are far from each other and the ICP falls into a local (not global) minimum, yielding an erroneous pose estimate
- 3) assuming scans are correctly pre-aligned using odometry or inertial sensor information such that the ICP identifies the global minimum, the displacement estimate will still possess uncertainty due to sensor noise and possibly underconstrained environments (such as a long featureless corridor).

The first two situations constitute the major sources of error for ICP. In those cases, finding the covariance of the computed displacement through a simple formula would be out of reach, and anyway would not be very meaningful as in those cases the ICP essentially fails. For these reasons, and because we are mainly motivated by navigation and EKF-SLAM purposes where we assume to have sufficiently accurate motion sensors, we focus on the third situation. Note that the pre-alignment assumption may still fail even with accurate motion sensors in the case of loop closure.

There have been various methods proposed to estimate the ICP covariance, see e.g. [7], [8] and references therein. Because of a lack of space, we refer the reader to [8] for more information about their potential shortcomings.

### B. Main message of the paper

The covariance of scan matching algorithms can be computed as follows [9], [8]. The estimated motion parameters  $\hat{x}$  output by the algorithm are defined as a local argmin of a cost function  $J(x, z)$  of the motion parameters  $x$  and the data  $z$  (scanned clouds). As a result we always have  $\frac{\partial}{\partial x} J(\hat{x}, z) \equiv 0$ . By the implicit function theorem  $\hat{x}$  is a function of the data  $z$  around this minimum. Roughly speaking, because of the identity above, a small variation  $\delta z$  in the data will imply a small variation  $\delta x$  in the estimate as  $\frac{\partial^2 J}{\partial x^2} \delta x + \frac{\partial^2 J}{\partial z \partial x} \delta z = 0$ , so that  $\delta x = -(\frac{\partial^2 J}{\partial x^2})^{-1} \frac{\partial^2 J}{\partial z \partial x} \delta z$ . As a result if  $\delta z$  denotes the (random) discrepancy in the measurement under the effect of sensor noise, according to the previous formula the corresponding variability in the

Silvère Bonnabel and François Goulette are with MINES ParisTech, PSL - Research University, Centre de robotique, 60 Bd St Michel 75006 Paris, France {firstname.lastname}@mines-paristech.fr

Martin Barczyk is with the Department of Mechanical Engineering, University of Alberta, Edmonton AB, T6G 2G8, Canada martin.barczyk@ualberta.ca

estimates writes  $\text{cov}(\hat{x}) := \mathbb{E}(\delta x \delta x^T)$ ,

$$\text{cov}(\hat{x}) := \left( \frac{\partial^2 J}{\partial x^2} \right)^{-1} \frac{\partial^2 J}{\partial z \partial x} \text{cov}(z) \frac{\partial^2 J}{\partial z \partial x}^T \left( \frac{\partial^2 J}{\partial x^2} \right)^{-1} \quad (1)$$

This is the closed-form expression proposed in [8] to approximate the ICP covariance. Our present goal is to point out the potential lack of validity of this formula for ICP covariance computation, but also to characterize situations where it can safely be used. Indeed, the problem with the formula is that it relies on the earlier identity  $\delta x = -\left(\frac{\partial^2 J}{\partial x^2}\right)^{-1} \frac{\partial^2 J}{\partial z \partial x} \delta z$ , which is based on the local implicit function theorem, and which proves to be only true for *infinitesimal variations*  $\delta x, \delta z$ . In the case of ICP, infinitesimal means sub-pixel displacements. Indeed when matching scans, the rematching step performed by the ICP makes the cost function far from smooth, so that the Taylor expansion

$$\frac{\partial J}{\partial x}(\hat{x} + \Delta x, z) = \frac{\partial J(\hat{x}, z)}{\partial x} + \frac{\partial^2 J(\hat{x}, z)}{\partial x^2} \Delta x + O(\Delta x^2) \quad (2)$$

which is true in the limit  $\Delta x \rightarrow 0$  may turn out to be *completely wrong* for displacements  $\Delta x$  larger than only a few pixels. This is typically what happens when applying (2) and thus (1) to the basic point-to-point ICP algorithm, as illustrated in Figures 1 and 2, which will be explained in greater detail in the sequel (Section II-A). Indeed we will see that in Figure 2, the dashed line displays the second-order Taylor approximation (2) to the ICP cost  $J(x, z)$ , whereas the solid line represents the true cost  $J(x, z)$  as the second cloud is moved to the right. They coincide for subpixel translations but soon diverge for larger ones. On the other hand, when the registration errors are projected onto the reference surface, as in point-to-plane ICP, Equation (1) can be justified by the results of Section III.

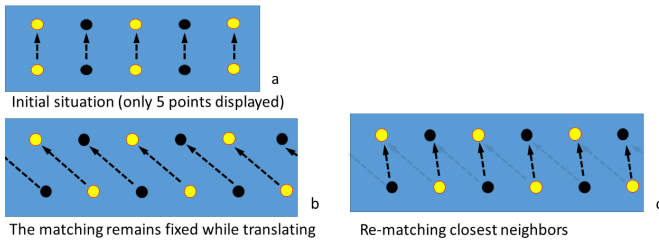


Fig. 1. Point-to-point ICP simple experimental setting. a) The first cloud is made of 10 equally spaced collinear points (i.e. scanned from a wall), the second cloud is obtained by duplication. To ensure overlap we focus on the central points. b) While translating the second cloud to the right, no re-matching occurs. c) Translation and re-matching with closest points. The costs  $J$  corresponding to cases b and c are shown in Fig. 2.

### C. Contributions and organization

Our paper is essentially an extension and rigorous justification of the results of [10] and [8]. Our main contributions are to point out the potential shortcomings of a blind application of the results of [10] and [8] to ICP variants in Section II, and then to provide a mathematical justification based on geometry arguments for the point-to-plane ICP in Section III. Finally the results are illustrated on a simple 3D case in Section IV.

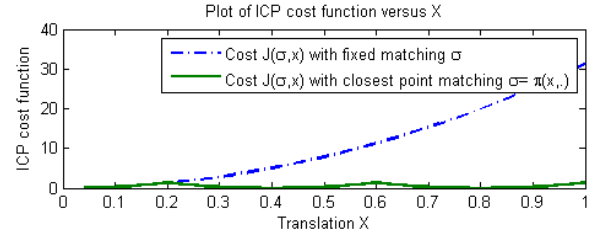


Fig. 2. Experimental setting of Fig. 1 case a. Plot of the second-order approximation to the cost  $J(\pi(\hat{X}, \cdot), \hat{X}) + 0 + \frac{\partial^2 J}{\partial X^2} J(\pi(\hat{X}, \cdot), \hat{X})(X - \hat{X})^2$  versus translations (dashed line). Due to the quadratic form of the cost (4) the second-order approximation is also equal to  $J(\pi(\hat{X}, \cdot), X)$ , i.e. the cost with matching held fixed (Fig 1 case b). Plot of the true ICP cost  $J(\pi(X, \cdot), X)$  (solid line), i.e. accounting for re-matching with closest points (Fig 1 case c).

## II. MATHEMATICAL FRAMEWORK

Following the notation of [8], the surface matching problem in 2D consists in finding the argmin  $\hat{X}$  of

$$J(S_r, \{p_k\}; X) := \sum_k \|Xp_k - \Pi(S_r, Xp_k)\|^2 \quad (3)$$

where  $S_r$  is a given reference surface in  $\mathbb{R}^2$ ,  $X$  is a displacement matrix such that the action of  $X$  on a vector  $Xp := Rp + T$  consists of a rotation followed by a translation,  $\{p_k\}$  is a cloud of points obtained by scanning the surface, and  $\Pi(S_r, \cdot)$  is the projection onto the surface  $S_r$ . The argmin  $\hat{X}$  is the solution to an optimization problem and is thus supposed to have covariance (1) according to e.g. [8].

Now consider using ICP for scan matching (either in 2D or 3D). In this case two clouds of points  $\{p_k\}_{1 \leq k \leq N}$  and  $\{q_i\}_{1 \leq i \leq M}$  are matched. The basic point-to-point ICP consists of the following steps which are iterated until convergence:

- for all  $k$  define  $\pi(k, X_{old})$  such that  $q_{\pi(k, X_{old})}$  is the point of the second cloud which is the closest to  $(X_{old})p_k$
- define  $X_{new}$  as the argmin of  $\sum_k \|Xp_k - q_{\pi(k, X_{old})}\|^2$

It is easy to see that the goal pursued is to minimize the function

$$J(\{p_i\}, \{q_i\}; \sigma, X) := \sum_k \|Xp_k - q_{\sigma(k)}\|^2 \quad (4)$$

over the roto-translation  $X$  and the matching  $\sigma : \{1, \dots, N\} \mapsto \{1, \dots, M\}$ . As a result, ICP appears as a *coordinate descent* which alternatively updates  $X$  as the argmin  $X$  of  $J$  for fixed  $\pi$ , and the argmin  $\pi$  of  $J$  for fixed  $X$  (the latter being true only for point-to-point ICP). This is what allows to prove local convergence, as done in the seminal paper [1]. Because of the huge combinatorial problem underlying the optimization problem of jointly minimizing  $J$  over the displacement and the matching, ICP provides a simple and tractable (although computationally heavy) approach to estimate the displacement. The ICP algorithm possesses many variants, such as the point-to-plane version

where the cost function is replaced with

$$J(\{p_i\}, \{q_i\}; \sigma, X) := \sum_k \|(Xp_k - q_{\sigma(k)}) \cdot n_{\sigma(k)}\|^2 \quad (5)$$

that is, the registration error is projected onto the surface unit normal vector of the second cloud at  $q_{\sigma(k)}$ . An alternative to this in 2D exploited in [8] consists of creating a reference surface  $S_r$  by connecting the points in the second cloud  $\{q_i\}$  with segments, and then employing cost function (3).

**Definition 1** *The closest point matching  $\pi(k, X)$  denotes the label  $j$  of the point  $q_j$  of the second cloud which is the closest to  $Xp_k$ .*

**Definition 2** *We define the ICP cost function as  $J(\{p_i\}, \{q_i\}; \pi(\cdot, X), X)$ , that is, the error function  $J(\{p_i\}, \{q_i\}; \sigma, X)$  with closest neighbor matching.*

**Definition 3** *The stability of the ICP in the sense of [10] is defined as the variation of the ICP cost function when  $X$  moves a little away from the argmin  $\hat{X}$ .*

Definition 3's terminology comes from the theory of dynamical systems. Indeed, the changes in the ICP cost indicate the ability (and speed) of the algorithm to return to its minimum when it is initialized close to it. If the argmin  $\hat{X}$  is changed to  $\hat{X} + \delta X$  and the cost does not change, then the ICP algorithm output will remain at  $\hat{X} + \delta X$  and will not return to its original value  $\hat{X}$ .

Meanwhile, although closely related, the covariance is rooted in statistical considerations and not in the dynamical behavior of the algorithm:

**Definition 4** *The covariance of the ICP algorithm is defined as the statistical dispersion (or variability), due to sensor noise, of the transformation  $\hat{X}$  computed by the algorithm over a large number of experiments.*

#### A. Potential lack of validity of (1)

1) *Mathematical insight:* Consider the ICP cost function  $J(\{p_i\}, \{q_i\}; \pi(X, \cdot), X)$ . To simplify notation we omit the clouds and we let  $F(X)$  be the function  $X \rightarrow J(\pi(X, \cdot), X)$ . At convergence we have by construction of the ICP algorithm as an argmin  $\partial_2 J(\pi(\hat{X}, \cdot), \hat{X}) = 0$ , where the  $\partial_2$  denotes the derivative with respect to the second argument. As the closest point matching  $X \rightarrow \pi(X, \cdot)$  is locally constant (except on a set of null measure), since an infinitesimal change of each point does not change the nearest neighbors except if the point is exactly equidistant to two distinct points, we have

$$\frac{d^2 F}{dX^2}(\hat{X}) = \partial_2^2 J(\pi(\hat{X}, \cdot), \hat{X})$$

that is, the matching can be considered as fixed when computing the Hessian of  $X \rightarrow J(\pi(X, \cdot), X)$  at the argmin. But the first-order approximation

$$\begin{aligned} \partial_2 J(\pi(\hat{X} + \delta X, \cdot), \hat{X} + \delta X) \\ \approx \partial_2 J(\pi(\hat{X}, \cdot), \hat{X}) + \partial_2^2 J(\pi(\hat{X}, \cdot), \hat{X}) \delta X \end{aligned}$$

can turn out to very poorly model the stability of the algorithm at the scale  $\delta X = \Delta X$  of interest to us, precisely because when moving away from the current argmin, rematching occurs and thus  $\pi(\hat{X} + \Delta X, \cdot) \neq \pi(\hat{X}, \cdot)$ .

Whereas a closed form estimate of  $\partial_2^2 J(\pi(\hat{X}, \cdot), \hat{X})$  is easy to calculate, obtaining a Taylor expansion around the minimum *which accounts for rematching* would require sampling the error function all around its minimum, leading to high computational cost [11], [12].

2) *Illustration on a simple example:* Consider the simple point-to-point ICP algorithm. Figures 1 and 2 illustrate the fallacy of considering a second-order Taylor expansion of the cost, i.e. computing the cost with fixed matching. Indeed, Fig. 2 displays the discrepancy between the true ICP cost and its second-order approximation around the minimum when moving along a featureless wall in 2D. We see that rematching with closest point correctly reflects the under-constraint/inobservability of the environment, since the cost function is nearly constant as we move along the featureless wall. On the other hand, the second-order approximation does not. This proves the Hessian  $\frac{\partial^2 J}{\partial X^2}$  to the cost at the minimum does not correctly reflect the change in the cost function value, and thus the stability of the algorithm.

Regarding covariance, it is easy to see that Equation (1) will not reflect the true covariance of the ICP either, as the true covariance should be very large (ideally infinite) along the wall's direction, which can only happen if  $\frac{\partial^2 J}{\partial X^2}$  is very small, but which is not the case here.

#### B. Covariance of least-squares

Consider the least-squares minimization problem

$$J(x) = \sum_i \|d_i - B_i x\|^2 \quad (6)$$

The solution is well known to be

$$\hat{x} = \left( \sum_i B_i^T B_i \right)^{-1} \left( \sum_i B_i^T d_i \right) \quad (7)$$

Let  $A := \left( \sum_i B_i^T B_i \right)$ , which represents the (half) Hessian  $\frac{1}{2} \partial_2^2 J$  of the cost function  $J$ . If the measurement  $d_i$  satisfies  $d_i = B_i x + w_i$  where  $x$  is the true parameter and  $w_i$  a noise, the covariance of the least squares estimate over a great number of experiments is of course given by

$$\begin{aligned} \text{cov}(\hat{x}) &= \mathbb{E} \left\langle A^{-1} \left( \sum_i B_i^T w_i \right) \left[ A^{-1} \left( \sum_j B_j^T w_j \right) \right]^T \right\rangle \\ &= A^{-1} \sum_i \sum_j \left( B_i^T \mathbb{E}(w_i w_j^T) B_j \right) A^{-1} \end{aligned} \quad (8)$$

which indeed agrees with (1). Furthermore, if the  $w_i$ 's are identically distributed independent noises with covariance matrix  $\mathbb{E}(w_i w_j^T) = \sigma^2 I \delta_{ij}$ , we recover the well-known result [13, Thm. 4.1] that

$$\text{cov}(\hat{x}) = \sigma^2 A^{-1} \left( \sum_i B_i^T B_i \right) A^{-1} = \sigma^2 A^{-1}$$

meaning the (half) Hessian to the cost function  $A$  encodes the covariance of the estimate.

### C. Application to point-to-point ICP

The application of the least-squares covariance formulas to point-to-point ICP can be done as follows as first proposed by [14] (to our best knowledge). In order to compute derivatives of the cost function with respect to the displacement estimate  $\hat{X}$ , we need to define differentiation with respect to a rotation matrix, a parameter which belongs to the Lie group  $SO(3)$ . This is a very well known problem which pertains to the realm of optimization on manifolds [15]. In our case, the solution boils down to approximating a small rotation with a cross product, i.e.  $Xp \approx p + x_R \times p + x_T$ . Thus in the sequel we consider the pose as parameterized by  $x = (x_R, x_T) \in \mathbb{R}^6$ .

Using the above approximation in the point-to-point ICP, the cost function (4) with matching fixed at its convergence value  $\hat{x}$  writes (around  $\hat{x}$ )

$$J(\pi(\hat{x}, \cdot), x) = \sum_i \|p_i + x_R \times p_i + x_T - q_{\pi(\hat{x}, i)}\|^2$$

which can be rewritten in the sum-of-squares form (6) with

$$d_i = p_i - q_{\pi(\hat{x}, i)}, \quad B_i = [S(p_i) \quad -I]$$

where  $S(\cdot)$  is the  $3 \times 3$  skew-symmetric matrix such that  $S(a)b = a \times b$ ,  $a, b \in \mathbb{R}^3$ . The Hessian  $\frac{1}{2}\partial_2^2 J = \sum_i B_i^T B_i$  is equal to

$$\sum_i \begin{bmatrix} -S(p_i)^2 & S(p_i) \\ -S(p_i) & I \end{bmatrix}$$

### D. Application to point-to-plane ICP

For point-to-plane ICP, the cost function (5) with matching fixed at its convergence value  $\hat{x}$  is given by

$$J(\pi(\hat{x}, \cdot), x) = \sum_i [(x_R \times p_i + x_T + p_i - q_{\pi(\hat{x}, i)}) \cdot n_{\pi(\hat{x}, i)}]^2$$

Using the scalar triple product circular property  $(a \times b) \cdot c = (b \times c) \cdot a$ , this can also be rewritten in form (6) with

$$d_i = n_{\pi(\hat{x}, i)}^T (p_i - q_{\pi(\hat{x}, i)}) \\ B_i = \begin{bmatrix} -(p_i \times n_{\pi(\hat{x}, i)})^T & -n_{\pi(\hat{x}, i)}^T \end{bmatrix}$$

and the Hessian  $\frac{1}{2}\partial_2^2 J = \sum_i B_i^T B_i$  is equal to

$$\sum_i \begin{bmatrix} (p_i \times n_{\pi(\hat{x}, i)})(p_i \times n_{\pi(\hat{x}, i)})^T & (p_i \times n_{\pi(\hat{x}, i)})n_{\pi(\hat{x}, i)}^T \\ n_{\pi(\hat{x}, i)}(p_i \times n_{\pi(\hat{x}, i)}) & n_{\pi(\hat{x}, i)}n_{\pi(\hat{x}, i)}^T \end{bmatrix}$$

The above expression — previously obtained in [10] — correctly models the Hessian of  $J(\{p_i\}, \{q_i\}; x, \pi(\hat{x}, \cdot))$ ; but it is not clear, as was seen in the case of point-to-point ICP by Figure 2, if it correctly captures the behavior of the true ICP cost function  $J(\{p_i\}, \{q_i\}; x, \pi(x, \cdot))$  around  $\hat{x}$ , and thus the stability of the algorithm. However this formula has been widely used by practitioners and can be justified by the results in the next section.

## III. A RIGOROUS MATHEMATICAL RESULT FOR POINT-TO-PLANE ICP

The present section is devoted to prove that as far as point-to-plane ICP is concerned, and contrarily to the point-to-point case, Equation (2) is indeed valid, even for large  $\Delta x$ . In fact, a bound on  $\Delta x$  depending on the curvature of the scanned surface is given, allowing to characterize the domain of validity of the formula. This novel result provides a rigorous framework to justify the widely used approximations of [10].

**Theorem 1** *Consider a 2D environment made of (an ensemble of disjoint) smooth surface(s)  $S_r$  having maximum curvature  $\kappa$ . Consider a cloud of points  $\{a_i\}$  obtained by scanning the environment. Consider the cost  $J(\pi(x, \cdot), x)$  obtained by matching the cloud  $\{a_i\}$  with the displaced cloud  $\{a_i\} + x_R \times \{a_i\} + x_T$  where  $x := (x_R, x_T)$  are the motion parameters. As 0 is a global minimum the gradient vanishes at  $x = 0$ . The following second-order Taylor expansion*

$$J(\pi(x + \Delta x, \cdot), x + \Delta x) \\ = J(\pi(0, \cdot), 0) + \partial_2^2 J(\pi(0, \cdot), 0) \|\Delta x\|^2 + O(\kappa \|\Delta x\|^3) \quad (9)$$

is valid for  $\Delta x$  sufficiently small, but large enough to let rematching occur.

Note that if the environment is made of disjoint planes, we have  $\kappa = 0$  and both cost functions agree *exactly*. The remainder of this section is devoted to the proof of the theorem, and a corollary proving the result remains true in 3D. The reader uninterested by the mathematical details is advised to skip directly to Section IV.

### A. Precise result

The proof of the theorem is based on the following more precise preliminary result.

**Proposition** *Consider the assumptions of Theorem 1. Around the minimum  $x = 0$  the cost with fixed matching*

$$J(\pi(0, \cdot), x) \\ = \sum_i [(a_i + x_R \times a_i + x_T - a_{\pi(0, i)}) \cdot n_i]^2$$

*differs from the true ICP cost in the following way*

$$J(\pi(x, \cdot), x) \\ = \sum_i [(a_i + x_R \times a_i + x_T - a_{\pi(x, i)}) \cdot n_i + \psi_i]^2$$

*where the approximation error  $\psi_i$  is already second order in the function arguments as  $|\psi_i| \leq 8\kappa(\|x_R \times a_i + x_T\|)^2$  as long as  $\kappa|s_i - s_{\pi(x, i)}| \leq 1$  where  $s_i$  and  $s_{\pi(x, i)}$  denote the curvilinear abscissae of the points  $a_i$  and  $a_{\pi(x, i)}$  along the surface  $S_r$ .*

To begin with, note that the condition  $\kappa|s_i - s_{\pi(x, i)}| \leq 1$  is independent of the chosen units as  $\kappa|s_i - s_{\pi(x, i)}|$  is dimensionless. To fix ideas about the validity condition, assume the environment is circular with an arbitrary radius. The above condition means that the Taylor expansion is

proved valid as long as the displacement yields a rematching with the nearest neighbor at most 1 rad ( $57.3^\circ$ ) along the circle from the initial point. We see this indicates a large domain of validity. Note that in case where the environment is a line both functions coincide exactly.

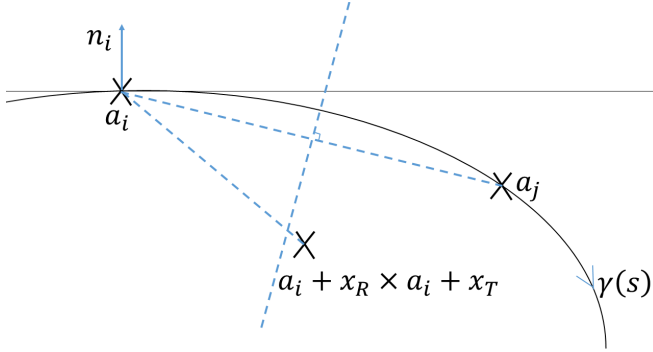


Fig. 3. Illustration for the proof.

To prove the result, assume the surface where point  $i$  lies is parameterized by  $\gamma(s)$  with curvilinear abscissa  $s$ , and with maximum curvature  $\kappa$ . Such a curve has tangent vector  $\gamma'(s)$  with  $\|\gamma'(s)\| = 1$  and normal vector  $\gamma''(s)$  with  $\|\gamma''(s)\| \leq \kappa$ , the curvature. The point cloud  $\{a_i\} \in \mathbb{R}^2$  is obtained by scanning this environment at discrete points  $\gamma(s_1), \gamma(s_2), \dots$ . We assume the surfaces (here curves) are sufficiently disjoint so that under the assumptions of the Proposition,  $a_i$  and its closest point  $a_{\pi(x,i)}$  lie on the same curve of maximum curvature  $\kappa$ . By writing  $x_R \times a_i + x_T + a_i - a_{\pi(x,i)} = x_R \times a_i + x_T + a_i - a_{\pi(0,i)} + a_{\pi(0,i)} - a_{\pi(x,i)}$  we see the error made for each term  $i$  is  $\psi := (a_{\pi(0,i)} - a_{\pi(x,i)}) \cdot n_i = (a_i - a_j) \cdot n_i$  where we let  $j := \pi(x,i)$  and we used the obvious fact that  $\pi(0,i) = i$ . To study  $\psi_i$  expand  $\gamma(s)$  about  $s = s_i$  using Taylor's theorem with remainder:

$$\gamma(s) = \gamma(s_i) + \gamma'(s_i)(s - s_i) + \int_{s_i}^s \gamma''(u)(u - s_i) du$$

Take  $s = s_{\pi(x,i)} := s_j$  and project along the normal  $n_i$ :

$$\begin{aligned} (\gamma(s_j) - \gamma(s_i)) \cdot n_i &= (s_j - s_i) \gamma'(s_i) \cdot n_i \\ &\quad + \int_{s_i}^{s_j} \gamma''(u) \cdot n_i (u - s_i) du \end{aligned}$$

Note  $\gamma'(s_i) \cdot n_i = 0$  since  $\gamma'(s_i)$  is the (unit) tangent vector to the curve at  $s = s_i$ . Taking absolute values of both sides,

$$\begin{aligned} |\psi_i| &= |(b_j - b_i) \cdot n_i| \leq \frac{1}{2} [\max_u \|\gamma''(u)\|] |s_j - s_i|^2 \\ &\leq \frac{1}{2} \kappa |s_j - s_i|^2 \\ &\leq \frac{1}{2} \kappa (4 \|x_R \times a_i + x_T\|)^2 \end{aligned}$$

as claimed. Only the last inequality needs be justified. It stems from the following result:

**Lemma** *If no rematching occurs, i.e.  $i = j$ , then  $\psi_i = 0$ . If  $i \neq j$ , we have for  $\kappa |s_i - s_j| \leq 1$  the inequality  $|s_i - s_j| \leq 4 \|x_R \times a_i + x_T\|$ .*

Indeed, rematching occurs only if the displaced point  $x_R \times a_i + x_T$  is closer to  $a_j$ , as illustrated in Fig. 3. But this implies the distance between the displaced point and  $a_i$  is greater than half the distance between  $a_i$  and  $a_j$  (see Fig. 3), that is  $\|a_j - a_i\| \leq 2 \|a_i + x_R \times a_i + x_T - a_i\|$ . Now, another Taylor expansion yields  $\gamma(s_j) - \gamma(s_i) = \gamma'(s_i)(s_j - s_i) + \int_{s_i}^{s_j} \gamma''(u)(u - s_i) du$ . Using  $\|\gamma'(s)\| = 1$  and  $\|\gamma''(s)\| \leq \kappa$  we get  $\|\gamma(s_j) - \gamma(s_i)\| \geq |s_j - s_i| - \frac{1}{2} \kappa (s_j - s_i)^2 \geq \frac{1}{2} |s_j - s_i|$ , the latter inequality stemming from the assumption that  $\kappa |s_j - s_i| \leq 1$ . Gathering those results we have thus proved

$$2 \|x_R \times a_i + x_T\| \geq \|a_j - a_i\| := \|\gamma(s_j) - \gamma(s_i)\| \geq \frac{1}{2} |s_j - s_i|$$

which allows to prove the Lemma, and in turn the Proposition.

### B. Extension to the 3D case

**Corollary** *The results hold in 3D where  $\kappa$  denotes the maximum of the Gauss principal curvatures.*

The corollary can be proved in exactly the same way as the theorem, by studying the discrepancy between both cost functions term-by-term. The idea is then merely to consider the plane spanned by the unit normal  $n_i$  and the segment relating  $a_i$  and  $a_j$ . This plane intersects the surface  $S_r$  at a curve, and the same process can be applied as in the 2D case. The curvature of this curve is by definition less than the maximum Gauss principal curvature of the surface.

## IV. ILLUSTRATION OF THE RESULTS IN 3D

The covariance of scan matching estimates is computed using Equation (8), which requires a model of the measurement noise  $w_i$  via its covariance  $\mathbb{E}(w_i w_i^T)$ . Modeling noise of a given sensor type is an entire subject on its own and will not be considered in the present paper. However it's clear from (8) that the Hessian  $A$  of the cost function plays a key role in this computation. We now demonstrate using a very simple numerical example in 3D that the Hessian of the point-to-plane correctly models the behavior of the algorithm.

Consider a 3D scan  $\{p_i\}$  of a plane wall by a facing scanner placed  $d$  units away as shown in Figure 4. A depth image of  $N_H$  by  $N_V$  pixels (function of the hardware) captures a surface measuring  $H$  by  $V$  units (function of the optical field of view and distance  $d$ ) such that  $a_i = [x_i \ y_i \ d]^T$  where  $-H/2 \leq x_i \leq H/2$ ,  $-V/2 \leq y_i \leq V/2$ .

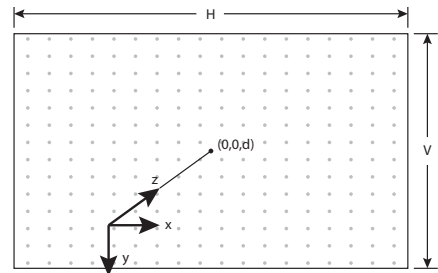


Fig. 4. Scan of 3D plane wall with  $N_H$  horizontal and  $N_V$  vertical points distributed symmetrically about origin.

Assume a previous scan  $\{q_i\}$  with associated surface normals  $\{n_i\}$  was captured with the same camera orientation at distance  $d'$  such that  $q_i = [x'_i \ y'_i \ d']^T$ ,  $n_i = [0 \ 0 \ -1]^T$  where  $-H'/2 \leq x'_i \leq H'/2$ ,  $-V'/2 \leq y'_i \leq V'/2$ . By Section II-D we have

$$A = \sum_i \begin{bmatrix} y_i^2 & -x_i y_i & 0 & 0 & 0 & y_i \\ -x_i y_i & x_i^2 & 0 & 0 & 0 & -x_i \\ 0 & 0 & 0 & 0 & 0 & 0 \\ 0 & 0 & 0 & 0 & 0 & 0 \\ 0 & 0 & 0 & 0 & 0 & 0 \\ y_i & -x_i & 0 & 0 & 0 & 1 \end{bmatrix} \\ = \begin{bmatrix} \Psi & 0 & 0 & 0 & 0 & 0 \\ 0 & \Xi & 0 & 0 & 0 & 0 \\ 0 & 0 & 0 & 0 & 0 & 0 \\ 0 & 0 & 0 & 0 & 0 & 0 \\ 0 & 0 & 0 & 0 & 0 & 0 \\ 0 & 0 & 0 & 0 & 0 & N \end{bmatrix}$$

where  $\sum x_i^2 := \Xi$ ,  $\sum y_i^2 := \Psi$  and  $\sum 1 := N$  are non-zero. By inspection this  $A$  possesses three zero eigenvalues with associated eigenvectors  $(e_3, e_4, e_5) \in \mathbb{R}^6$ , indicating that in this case rotations about the  $z$  axis and translations along the  $x$  and  $y$  axes are unobservable to scan matching, which agrees with physical intuition about Figure 4. Although  $A$  is singular, (8) can still be computed by removing  $x_3$ ,  $x_4$  and  $x_5$  from the state vector  $x = [x_R \ x_T]$ , thus deleting the 3<sup>rd</sup>, 4<sup>th</sup> and 5<sup>th</sup> column of  $B_i$  or rows and columns of  $A$ . In this way only the covariance of observable parameters will be estimated.

Now consider using the point-to-point Hessian given in Section II-C. In this case we have

$$A = \sum_i \begin{bmatrix} d^2 + y_i^2 & -x_i y_i & -d x_i & 0 & -d & y_i \\ -x_i y_i & d^2 + x_i^2 & -d y_i & d & 0 & -x_i \\ -d x_i & -d y_i & x_i^2 + y_i^2 & -y_i & x_i & 0 \\ 0 & d & -y_i & 1 & 0 & 0 \\ -d & 0 & x_i & 0 & 1 & 0 \\ y_i & -x_i & 0 & 0 & 0 & 1 \end{bmatrix} \\ = \begin{bmatrix} Nd^2 + \Psi & 0 & 0 & 0 & -N & 0 \\ 0 & Nd^2 + \Xi & 0 & Nd & 0 & 0 \\ 0 & 0 & \Xi + \Psi & 0 & 0 & 0 \\ 0 & Nd & 0 & N & 0 & 0 \\ -Nd & 0 & 0 & 0 & N & 0 \\ 0 & 0 & 0 & 0 & 0 & N \end{bmatrix}$$

By inspection this  $A$  is full rank and so it does not have zero eigenvalues. Since we know there are three unobservable directions, the point-to-point ICP Hessian provides an incorrect model of the scan matching observability (and in turn covariance), exactly as predicted.

## V. CONCLUSIONS

In this paper we have provided a rigorous mathematical result proving the closed-form expression (1) appearing in [8], [10], when employed with point-to-plane ICP, is valid provided our formulated assumptions hold. We have also formally justified — a novel result to our best knowledge — why (1) is not valid for application to point-to-point ICP.

The Appendix presents preliminary results about sensor error modeling of a Kinect camera. In the future we plan to further investigate this sensor's error modeling in order to obtain a valid and realistic covariance matrix for scan matching applications.

## ACKNOWLEDGMENTS

The work reported in this paper was partly supported by the Cap Digital Business Cluster TerraMobilita Project.

## REFERENCES

- [1] P. J. Besl and N. D. McKay, "A method for registration of 3-D shapes," *IEEE Transactions on Pattern Analysis and Machine Intelligence*, vol. 14, no. 2, pp. 239–256, February 1992.
- [2] Y. Chen and G. Medioni, "Object modelling by registration of multiple range images," *Image and Vision Computing*, vol. 10, no. 3, pp. 145–155, April 1992.
- [3] F. Lu and E. E. Milios, "Robot pose estimation in unknown environments by matching 2D range scans," in *Proceedings of the 1994 IEEE Computer Society Conference on Computer Vision and Pattern Recognition*, Seattle, WA, June 1994, pp. 935–938.
- [4] G. Grisetti, R. Kummerle, C. Stachniss, and W. Burgard, "A tutorial on graph-based SLAM," *Intelligent Transportation Systems Magazine, IEEE*, vol. 2, no. 4, pp. 31–43, 2010.
- [5] J. Nieto, T. Bailey, and E. Nebot, "Recursive scan-matching SLAM," *Robotics and Autonomous Systems*, vol. 55, no. 1, pp. 39–49, January 2007.
- [6] A. Mallios, P. Ridaou, D. Ribas, F. Maurelli, and Y. Petillot, "EKF-SLAM for AUV navigation under probabilistic sonar scan-matching," in *Proceedings of the 2010 IEEE/RSJ International Conference on Intelligent Robots and Systems*, Taipei, Taiwan, October 2010, pp. 4404–4411.
- [7] O. Bengtsson and A.-J. BaerVELdt, "Robot localization based on scan-matching — estimating the covariance matrix for the IDC algorithm," *Robotics and Autonomous Systems*, vol. 44, no. 1, pp. 29–40, July 2003.
- [8] A. Censi, "An accurate closed-form estimate of ICP's covariance," in *Proceedings of the 2007 IEEE International Conference on Robotics and Automation*, Roma, Italy, April 2007, pp. 3167–3172.
- [9] A. K. R. Chowdhury and R. Chellappa, "Stochastic approximation and rate-distortion analysis for robust structure and motion estimation," *International Journal of Computer Vision*, vol. 55, no. 1, pp. 27–53, 2003.
- [10] S. Rusinkiewicz. ICP stability. [Online]. Available: <http://www.cs.princeton.edu/~srs/papers/icpstability.pdf>
- [11] P. Biber and W. Strasser, "The normal distributions transform: a new approach to laser scan matching," in *Proceedings of the 2003 IEEE/RSJ International Conference on Intelligent Robots and Systems*, Las Vegas, NV, October 2003, pp. 2743–2748.
- [12] J. Nieto, T. Bailey, and E. Nebot, "Scan-SLAM: Combining EKF-SLAM and scan correlation," in *Field and Service Robotics: Results of the 5th International Conference*, ser. Springer Tracts in Advanced Robotics, P. Corke and S. Sukkarieh, Eds. Berlin: Springer, 2006, vol. 25, pp. 167–178.
- [13] S. M. Kay, *Fundamentals of Statistical Signal Processing: Estimation Theory*. Prentice Hall, 1993.
- [14] O. Bengtsson and A.-J. BaerVELdt, "Localization in changing environments — estimation of a covariance matrix for the IDC algorithm," in *Proceedings of the 2001 IEEE/RSJ International Conference on Intelligent Robots and Systems*, Maui, Hawaii, USA, October 2001, pp. 1931–1937.
- [15] P.-A. Absil, R. Mahony, and R. Sepulchre, *Optimization algorithms on matrix manifolds*. Princeton University Press, 2009.
- [16] K. Khoshelham and S. Oude Elberink, "Accuracy and resolution of Kinect depth data for indoor mapping applications," *Sensors*, vol. 12, no. 2, pp. 1437–1454, February 2012.
- [17] S. Rusinkiewicz and M. Levoy, "Efficient variants of the ICP algorithm," in *Proceedings of the Third International Conference on 3-D Digital Imaging and Modeling*, Quebec City, Canada, May 2001, pp. 145–152.

APPENDIX

PRELIMINARY RESULTS ON KINECT ERROR MODELING

In order to evaluate (8) we require to assume a model on the noise terms  $w_i$  in the measurement model  $d_i = B_i x + w_i$ . Employing the point-to-plane terms from Section (II-D) with  $\pi(\hat{x}, i) \equiv i$  as  $d_i = n_i^T(p_i - q_i)$ ,  $B_i = [-(p_i \times n_i)^T \quad -n_i^T]$  yields

$$\begin{aligned} w_i &= n_i^T(p_i - q_i) + (p_i \times n_i)^T x_R^* + n_i^T x_T^* \\ &= [(x_R^* \times p_i) + x_T^* + p_i - q_i] \cdot n_i := r_i \cdot n_i \end{aligned}$$

where  $r_i \in \mathbb{R}^3$  represents the post-alignment error of the  $i^{\text{th}}$  point pair due to sensor error. The noise  $w_i = r_i \cdot n_i = n_i^T r_i$  thus represents the projection of  $r_i$  and (8) becomes

$$\text{cov}(\hat{x}) = A^{-1} \sum_i \sum_j \left( B_i^T n_i^T \mathbb{E}(r_i r_j^T) n_j B_j \right) A^{-1} \quad (10)$$

A. Random Noise Errors

A natural approach is to assume the post-alignment errors  $r_i$  are independent and identically normally isotropically distributed as

$$r_i \sim \mathcal{N}(0, \sigma^2 I_3) \quad (11)$$

Under these assumptions  $E\langle r_i r_j^T \rangle = E\langle r_i \rangle E\langle r_j^T \rangle = 0$ ,  $i \neq j$  and the double sum in (10) reduces to a single sum ( $n_i^T n_i = 1$  for unit normals):

$$\text{cov}(\hat{x}) = A^{-1} \sigma^2 \sum_i B_i^T B_i A^{-1} = \sigma^2 A^{-1} \quad (12)$$

as stated in Section II-B. However (12) would provide *unrealistically optimistic* results. Recall the simple 3D example in Section IV in the point-to-plane case. Matrix  $A$  is singular and so (12) cannot be evaluated. However we can proceed by removing  $x_3$ ,  $x_4$  and  $x_5$  from the state vector  $x = [x_R \quad x_T]$ , thus deleting the 3<sup>rd</sup>, 4<sup>th</sup> and 5<sup>th</sup> rows and columns of  $A$  such that we work with the subspace of observable parameters. We have

$$\Xi = \sum x_i^2 = 2 \sum_{k=1}^{N_H/2} \left( \frac{kH}{N_H} \right)^2 = \frac{H^2(N_H+1)(N_H+2)}{12N_H}$$

and  $\Psi = \sum y_i^2$  is obtained by replacing  $H$  and  $N_H$  with  $V$  and  $N_V$  respectively. Equation (12) becomes

$$\text{cov}(\hat{x}) = \sigma^2 \begin{bmatrix} \frac{12N_V}{V^2(N_V+1)(N_V+2)} & 0 & 0 \\ 0 & \frac{12N_H}{H^2(N_H+1)(N_H+2)} & 0 \\ 0 & 0 & \frac{1}{N} \end{bmatrix}$$

Consider parameter values representative of a Kinect. Assume  $d = 2$  m for which  $\sigma \approx 1$  cm [16, Fig. 10]. The Kinect has a field of view of  $57^\circ$  horizontally and  $43^\circ$  vertically such that  $H = 4 \tan 28.5^\circ \approx 2.17$  m,  $V = 4 \tan 21.5^\circ \approx 1.58$  m, and its depth images have  $N_H = 640$ ,  $N_V = 480$ . We obtain the standard deviations

$$\sqrt{\text{diag}(\text{cov}(\hat{x}))} = [0.06^\circ \quad 0.04^\circ \quad 0.02 \text{ mm}]$$

It is clear that the computed results are several orders of magnitude too optimistic — it is simply impossible to obtain displacement estimates with sub-millimeter precision by scan

matching images from a low-cost Kinect scanner. The reason is that the independent Gaussian noise (11) which models random errors becomes a negligible effect as the number of scanned points increases. We thus need to focus on a different noise effect, namely resolution errors of the scanner.

B. Resolution Errors

Suppose that  $N$  point pairs  $\{(p_i, q_i)\}$  are scanned and that the environment consists of  $K$  planes represented as disjoint subsets  $M_1, M_2, \dots, M_K$  of these pairs. We will assume the post-alignment errors  $r_i$  created by resolution errors are correlated with each other on a given plane  $M_k$  but independent of the other planes and among scanner axes, and denote the average axial resolution by  $\delta$ , such that

$$E\langle r_i r_j^T \rangle = \delta^2 I_3 \mathbf{1}_{M_k \times M_k}(i, j) \quad (13)$$

where  $\mathbf{1}$  is the indicator function defined as

$$\mathbf{1}_M(x) = \begin{cases} 1 & \text{if } x \in M, \\ 0 & \text{if } x \notin M. \end{cases}$$

Using (13), equation (10) becomes

$$\text{cov}(\hat{x}) = \delta^2 A^{-1} \sum_i \sum_j \left( B_i^T B_j \mathbf{1}_{M_k \times M_k}(i, j) \right) A^{-1} \quad (14)$$

Expanding the definition of  $B_k$  and denoting  $M_k \ni \{n_i\} := n_k$  as the normal of a given plane and  $N_k$  as the number of point pairs in subset  $M_k$ , the double sum in (14) becomes

$$\sum_k \sum_{i \in M_k} \begin{bmatrix} (p_i \times n_k)(\sum_{j \in M_k} p_j \times n_k)^T & (p_i \times n_k)N_k n_k^T \\ n_k(\sum_{j \in M_k} p_j \times n_k)^T & n_k N_k n_k^T \end{bmatrix}$$

and  $A$  can be expressed as

$$A = \sum_k \sum_{i \in M_k} \begin{bmatrix} (p_i \times n_k)(p_i \times n_k)^T & (p_i \times n_k)n_k^T \\ n_k(p_i \times n_k)^T & n_k n_k^T \end{bmatrix}$$

In principle (14) computes the covariance of  $\hat{x}$ , although it is unwieldy to use. We can simplify by assuming that all planes  $M_k$  are sufficiently compact such that the mean  $(1/N_k) \sum_{j \in M_k} p_j \approx p_i \in M_k$ . Under this assumption the double sum in (14) simplifies to

$$\sum_k N_k \sum_{i \in M_k} \begin{bmatrix} (p_i \times n_k)(p_i \times n_k)^T & (p_i \times n_k)n_k^T \\ n_k(p_i \times n_k)^T & n_k n_k^T \end{bmatrix}$$

Finally by assuming  $N_k = N/K$  i.e. each plane contains the same number of points, we obtain a much simpler version of (14):

$$\text{cov}(\hat{x}) = \delta^2 \frac{N}{K} A^{-1} = \delta^2 \frac{N}{K} \left( \sum_i B_i^T B_i \right)^{-1} \quad (15)$$

The assumption of planes  $M_k$  having the same number of points can be met by implementing normal space directed sampling [17] in the ICP algorithm. This consists of bucketing the computed normals of a scan based on their direction in angular space then sampling evenly across these buckets. Typically, in a standard room, one can implement the formula as an approximation to the true covariance by letting  $K = 5$ ,

that is the image is essentially made of three visible walls, roof and floor.

We return to the Section IV example of scan matching a plane wall. Since there is only one plane  $K = 1$ . Referring to the previous section, (15) yields

$$\text{cov}(\hat{x}) = \delta^2 N \begin{bmatrix} \frac{12N_V}{V^2(N_V+1)(N_V+2)} & 0 & 0 \\ 0 & \frac{12N_H}{H^2(N_H+1)(N_H+2)} & 0 \\ 0 & 0 & \frac{1}{N} \end{bmatrix}$$

Taking  $\delta = 0.01$  m as the resolution error of the Kinect at  $d = 2$  m [16, Fig. 10] gives

$$\sqrt{\text{diag}(\text{cov}(\hat{x}))} = [31.8^\circ \quad 20.0^\circ \quad 1 \text{ cm}]$$

which are much more reasonable numbers for Kinect scan matching performance at a 2 m distance.